Summer 2023

Groundwater Flow and Salt Marsh Migration: The Forest/Marsh Boundary

Camille Rossiello

Groundwater Flow and Salt Marsh Migration: The Forest/Marsh Boundary

By

Camille Rossiello

Bachelor of Arts
SUNY Purchase College, 2018

Submitted in Partial Fulfillment of the Requirements

For the Degree of Master of Science in

Geological Sciences

College of Arts and Sciences

University of South Carolina

2023

Accepted by:

Alicia Wilson, Director of Thesis

Jay Pinckney, Reader

Steven Pennings, Reader

Ann Vail, Dean of the Graduate School

ACKNOWLEDGEMENTS

I would like to express my sincere gratitude to my advisor, Dr. Alicia Wilson, for her guidance and constant support throughout my master's program. I would also like to thank Dr. Steven Pennings and Dr. Jay Pinckney for serving as my readers and providing helpful feedback.

I am grateful the National Science Foundation (Grant No. 1832178) for providing me the opportunity to complete my research at the Georgia Coastal Ecosystems Long-Term Ecological Research division and for all their resources. I would also like to extend thanks to Adam Sapp, John Williams, and other field technicians with assistance collecting data and providing online help.

Finally, I would like to thank my family as well as friends and colleagues at the University of South Carolina in the School of Earth, Ocean, and Environment (SEOE) for their motivation and unwavering support.

ABSTRACT

Salt marshes migrate landward in response to sea level rise, but the rate of this migration is not constant and can be influenced by pulse disturbances. Long term observations at Sapelo Island, Georgia, show that salt marsh migration has occurred during droughts, but the mechanism for this migration is unclear. Drought is thought to influence salt marsh migration by reducing fresh groundwater discharge from the upland. Rising sea level also encroaches on the upland, which could cause movement of the freshwater lens inland. A two-dimensional numerical model was built to simulate groundwater flow and solute transport based on the Marsh Landing marsh at Sapelo Island. The model is designed to estimate salinity changes in response to climatic factors, such as drought and sea level rise. After calibration against hydraulic head and salinity data from 2016-2020, the model was used to estimate salinity and movement of the freshwater lens through the forest/marsh boundary over a 25-year period from 1998-2022 that corresponds with plant community observations at the site. Observing the changes in salinity shows drought influences seasonal variations and sea level rise caused an overall increase in salinity near the forest marsh boundary.

TABLE OF CONTENTS

LIST OF TABLES

LIST OF FIGURES

CHAPTER 1: INTRODUCTION

Salt marshes are important coastal ecosystems. These intertidal wetlands provide significant ecosystem services including sequestration of carbon, nutrient transportation, and nursery habitat (Kirwan and Megonigal, 2013). While salt marshes have maintained an equilibrium in the past, disturbances can affect the ability of salt marshes to self-stabilize. Salt marsh migration, or a landward movement of the upper boundary of a salt marsh, can vary depending on different processes. An increased rate of sea level rise or a change in soil conditions due to groundwater salinity will affect plant zone distribution (Morris et al. 2002, Moffett et al. 2012, Burns et al. 2021).

Groundwater flow and salinity are important influences on ecological zonation in the salt marsh (Moffett et al. 2012, Wilson et al. 2015). Under unaltered marsh conditions, salt marsh migration of ecological zones depends on the rate of sea level rise and extent of high salinity zones (Pennings and Callaway 1992). Migration can be affected by the duration and intensity of extreme or acute pulse disturbances, such as high salinity, or by persistent, long term press disturbances, including sea level rise (Li and Pennings 2019). Quantifying the links between hydrology and salt marsh migration has been difficult because long-term plant monitoring has not typically been accompanied by observations of soil salinity, but recent work suggests that trends in salinity variations from disturbance or seasonality can be determined using numerical models. Numerical

groundwater models are useful in determining salt transport and salt marsh migration due to salinity (Moffett et al. 2012, Xiao et al. 2019). The combination of model simulations and knowledge of disturbance conditions can assist in predicting plant migration patterns in salt marshes.

1.1 Ecological Zonation of Salt Marshes in the Southeastern U.S.

Characteristic features of a salt marsh include zones of marsh plants that typically correlate with elevation and distance from a tidal creek inland (Figure 1.1). The most common plant found in the South-Eastern USA in the low and middle marsh areas is *Spartina alterniflora* (henceforth referred to as *Spartina*), while *Juncus roemerianus* (henceforth referred to as *Juncus*) dominates the high marsh near the freshwater upland (Pennings et al. 2005). Hypersaline zones commonly develop between areas of *Spartina* and *Juncus*. These zones may appear as salt flats or may be colonized by *Salicornia virginica* and *Batis maritima* (Figure 1.1, Pennings and Richards 1998).

The zonation that occurs in the marsh is strongly influenced by ecological competition and the tolerance of plants to stresses that include salinity and frequency of soil saturation (Pennings et al, 2005, Pennings and Callaway 1992). *Spartina* was shown to thrive in study plots with less competition when other plant species were removed while *Juncus* is limited by stress caused by salinity. The saturation of the soil as well as salinity are controlled by groundwater flow, which is in turn influenced by tidal fluctuations and precipitation events (Xin et al. 2010). Subregions within a salt marsh can

be categorized as different ecohydrological zones with varied conditions including salinity, saturation, or groundwater velocity (Moffett et al. 2012).

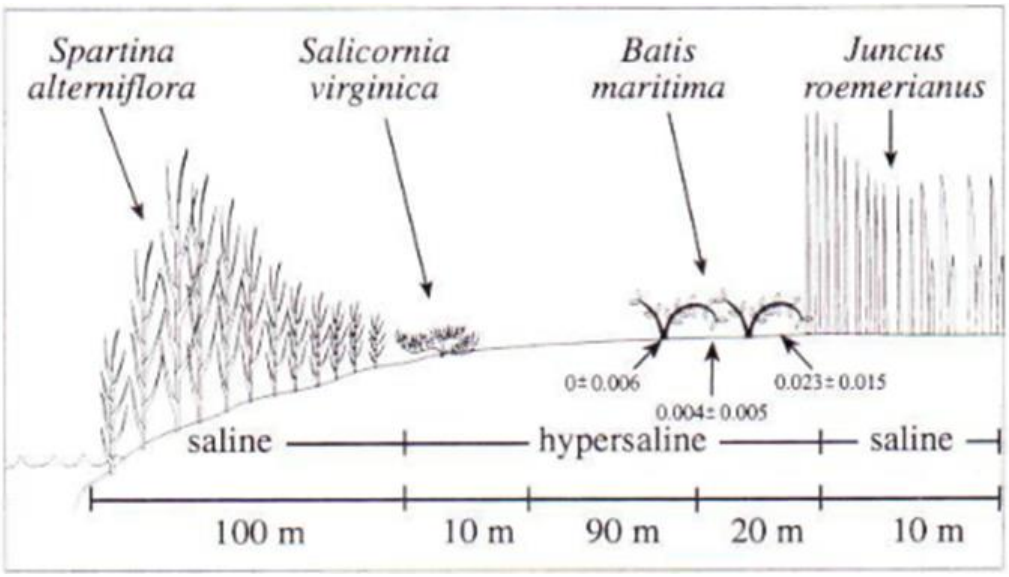

Figure 1.1- Salt marsh plant zonation at Sapelo Island, GA (Pennings and Richards 1998).

1.2 Groundwater Flow Through Salt Marshes

Groundwater flow in salt marshes is primarily influenced by tides and precipitation. Tidal fluctuations are the main drivers of groundwater flow in the low marsh shown by horizontal movement of water and salt throughout caused by ebb and flow of daily tides. Since the marsh platform is typically capped by a low-permeability mud layer, the saltwater takes longer to flow through that system causing vertical flow near the root zone in the low marsh. Vertical infiltration of fresh rainwater into the upland creates a freshwater lens and drives subsurface flow of fresh groundwater toward the

marsh, creating a freshwater-saltwater interface that migrates depending on precipitation rates (Wilson et al. 2015; Figure 1.2).

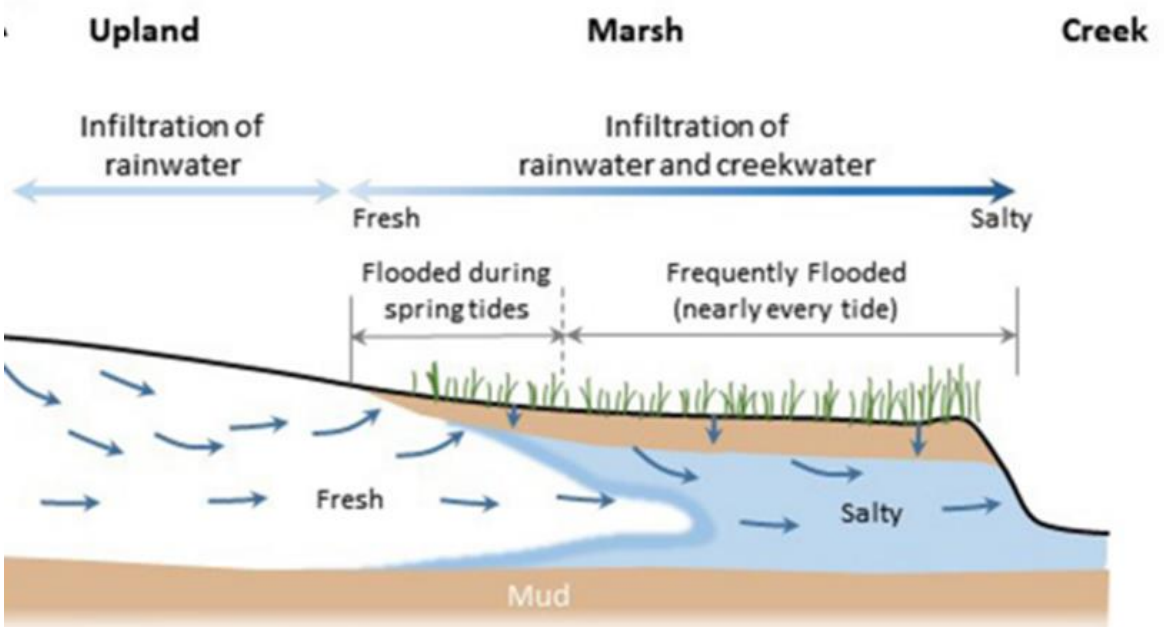

Figure 1.2: Conceptual model of groundwater flow through a salt marsh. Arrows indicate groundwater flow (Wilson et al. 2021).

Salinity can vary throughout different zones of the salt marsh. Southeastern salt marshes are inundated by semidiurnal tides in the low marsh, and higher zones of the marsh experience periodic cycles of flooding and exposure from spring and neap tides. There is increased solute transport, mainly salt, across the marsh during the recharge and drainage times which causes a fluctuation in salinity (Wilson and Gardner 2006, Wilson et al. 2015). Rainfall is one of the leading causes of salinity changes in the high marsh. This is caused by direct infiltration of rainwater into the marsh surface and freshwater discharge from the upland (Hughes et al. 2012). Evapotranspiration also contributes to variation in the porewater salinity in the high marsh (Miklesh and Meile 2018).

Variability in salinity at the forest/marsh boundary is difficult to predict or capture using simple 1-D models due to coupled responses from both tides and rainfall. Salinity in the low marsh zone of the marsh can be approximated using simple mass balance models (Morris 1995, Miklesh and Meile 2018).

The designated high marsh area is susceptible to changes from both short and long-term disturbances including sea level rise and migration of the freshwater lens. The marsh edge or low marsh can migrate due to erosion or human influence, causing just a decrease or increase of low marsh area. In comparison, with sea level rise the high marsh will migrate upslope overtaking upland area creating an expansion of the salt marsh. The change in low marsh area is controlled mainly by tidal conditions while migration in the high marsh depends on tidal conditions, slope of the marsh, human development, and climatic conditions (Burns et al. 2021, Fagherazzi et al. 2013). Emphasizing high marsh migration enables a focus on numerous disturbances. A pulse disturbance of varied dry or wet conditions can result in a contraction or expansion of the freshwater lens at the forest/marsh boundary (Figure 1.3 a,b). A press disturbance of sea level chronically increasing can also result in an upward vertical shift of the water table (Figure 1.3c). These conceptual controls on salinity and freshwater availability can vary based on actual climatic conditions and the dynamics of individual plant species in a salt marsh.

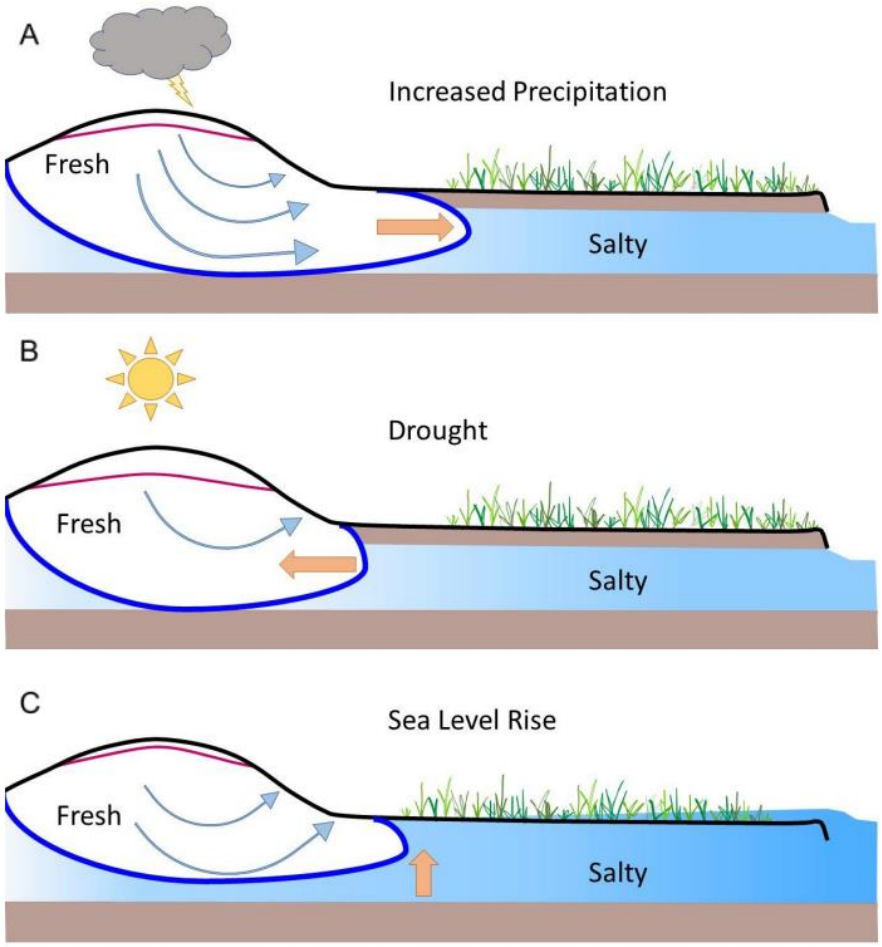

Figure 1.3: Conceptual model for groundwater flow and salinity in marshes with press and pulse disturbances. The water table is represented by the pink line in all figures. (a) Pulse disturbance with increased precipitation shown with lengthening of the freshwater lens with freshwater discharge towards the marsh. (b) Pulse disturbance of drought with contraction of the freshwater lens and decreased water level. (c) Press disturbance with steady increase in sea level showing an increase of salt water and migration of the freshwater lens up.

1.3 Field Evidence for Disturbance

Previous studies have investigated the connections between hydrology and changes in salt marshes. Solohin et al (2020) compared the effect of press and pulse

disturbances on the salinity of the root zone. The consistent press plots were designed to simulate gradual saltwater intrusion while the infrequent pulse plots simulated a short-term drought. The press disturbance demonstrated an increase in salinity and a leveling out at a high value for the rest of the experiment. Salinity increased and remained in high concentration throughout the experiment in the press plots while the pulse plots indicated only increase in salinity during the pulse treatment. The results show a significant decrease in nutrient availability and plant belowground biomass during press disturbance yet not during pulses. This suggested that sea level rise is more likely to influence long term plant migration than brief 2-month drought (Solohin et al. 2020).

A long-term study done at the Georgia Coastal Ecosystems Long Term Ecological Research network (GCE LTER) on Sapelo Island, GA suggested instead that vegetation migration is closely related to precipitation. Plant cover in study plots was recorded for 22 years, including three significant drought periods shown in 1998-2003, 2006-2009, and 2010-2013 (Figure 1.4). The drought conditions initiated an overall decrease in percent cover of *Juncus* with a simultaneous increase of *Batis* and *Salicornia* occurring three years into the 1998 drought and two years into the 2006 drought (Li and Pennings, 2019). Another study investigated the possibility that acute salt marsh dieback in the *Spartina* zone could be caused by increases in salinity and dry conditions during drought. Although *Spartina* is a saline-tolerant plant, it can experience dieback or change in steady state with an increase of salinity, specifically in 2001 during the 1998-2003 drought (Hughes et al. 2012).

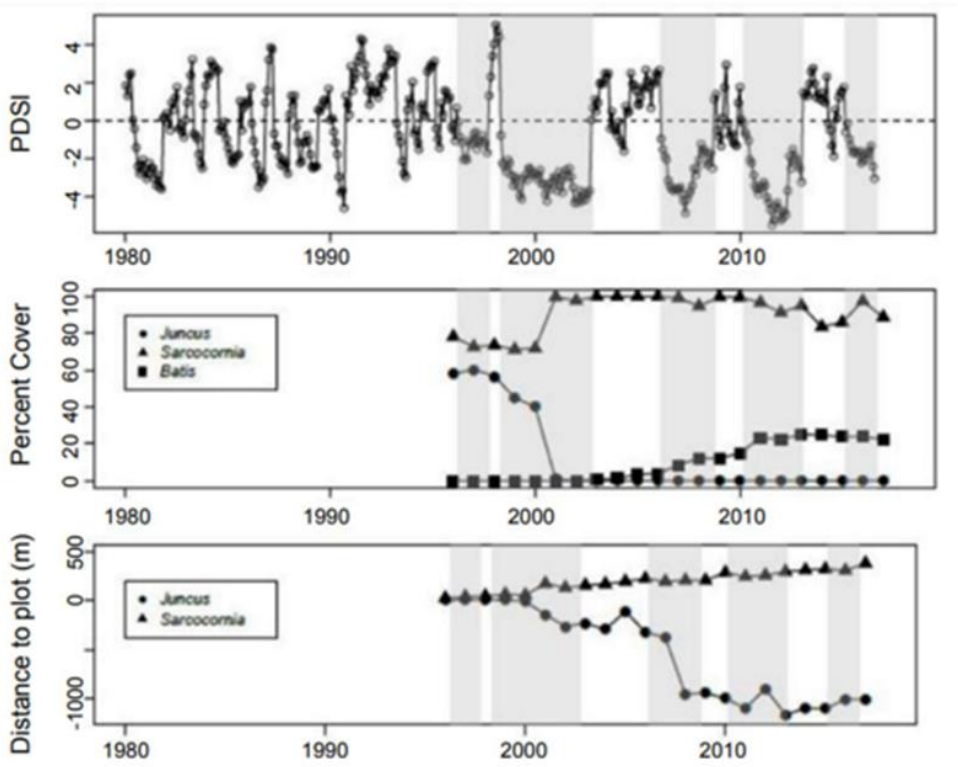

Figure 1.4. Marsh species response to drought(a) Palmer Drought Severity Index, (b) percent cover by vegetation averaged over 8 plots, (c) distance to plots over time measured from the middle of the plot to the edge of the plant zone. Negative values reflect plant retreat, positive values reflect plant advancement (Courtesy of S.C. Pennings).

These studies raise questions about how drought affects conditions in the root zone. The flourishing of saline tolerant plants *Batis* and *Salicornia* during an extended, intense drought (Figure 1.4; Li and Pennings 2019) indicates an increase of salinity, but this could have been caused by less infiltration of rainfall into the marsh surface, movement of freshwater lens towards the upland caused by less freshwater availability, or increased soil aeration. The overall goal of this study was to develop a predictive model for groundwater flow to interpret the salinity and flow patterns in response to disturbance over a 25-year period. The calibrated model was used to compare connections between salinity and freshwater lens migration with plant migration.

1.4 Study Area

This study was conducted at Marsh Landing, a salt marsh located on Sapelo Island. The long-term ecological monitoring research project established by the GCE-LTER provided us with decades of plant migration studies to be used as a baseline for this research. As previously described, droughts have coincided with migration of ecological zonation at this site (Figure 1.2). The groundwater changes associated with drought and sea level rise have not yet been explored.

Sapelo Island is a barrier island in McIntosh County, Georgia. The salt marsh where our data were collected is representative of typical low-latitude salt marshes in the Southeast US. The upland adjacent to this salt marsh is roughly 500 m across. Three monitoring wells were installed in a 50 m transect spanning the high marsh-upland boundary at the Marsh Landing marsh in 2018. The site is along the Duplin River to the north of the ferry dock (Figure 1.5).

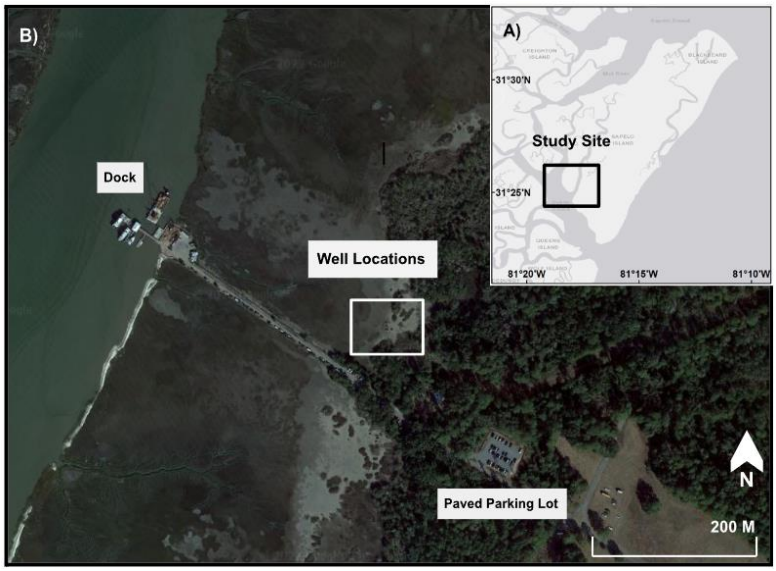

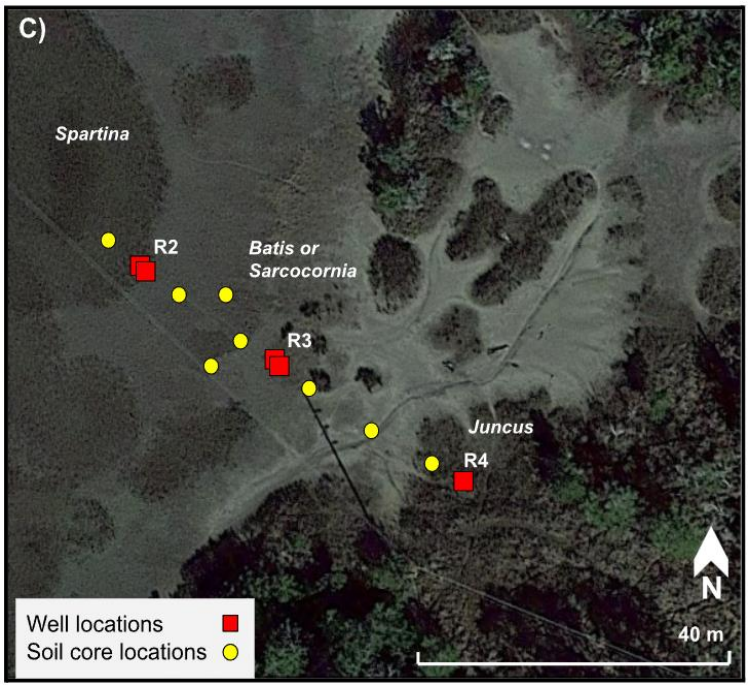

Figure 1.5: (a) Sapelo Island, GA. (b) Marsh Landing site. (c) Wells, soil cores, and plant zones in the high marsh at Marsh Landing.

The creekward-most well was installed about 440 m from the Duplin River. The furthest landward well is located about 500 m from the river, at the approximate forest-marsh boundary (Sanders 2021). The elevation increases from northwest to southeast (Table 1.1: Sanders 2021).

Table 1.1: Coordinates and elevation changes of monitoring wells (Sanders 2021).

Logger	Land surface elevation (m)	Logger elevation (cm)	Screen elevation (cm)	Latitude	Longitude
R2A	1.004	110.4	30.4	31°25'00.97916"N	81°17'34.99256"W
R2B	0.994	109.4	-20.6	31°25'00.95927"N	81°17'35.00630"W
R3A	1.07	117	47	31°25'00.64411"N	81°17'34.36862"W
R3B	1.047	114.7	-10.3	31°25'00.63045"N	81°17'34.38655"W
R4	1.449	154.9	-5.1	31°25'00.06366"N	81°17'33.42560"W

CHAPTER 2: METHODS

2.1 Preliminary Groundwater Model

Sanders (2021) developed a numerical model developed based on Marsh Landing to simulate groundwater flow and salinity at the marsh-forest boundary. Monitoring wells were installed in 2018 and sediment stratigraphy determined by hand augering at and near the wells with further extrapolation through the model domain based on common southeastern salt marsh stratigraphy (Gardner and Porter 2001, Wilson et al. 2011). Hydraulic head and salinity data gathered from monitoring wells were used to calibrate the model. The model was constructed using the method of Evans and Wilson (2015), who adapted SUTRA 2D3D (Voss and Provost, 2002) to incorporate changing boundary conditions, including changing tidal flooding and precipitation events (Wilson and Gardner, 2006).

The model simulated flow in a vertical cross section through Marsh Landing (Figure 1.5). The topography and elevation were estimated using LIDAR data and a digital elevation model from ArcGIS. Elevation discrepancies caused by trees were calculated from real time kinematic (RTK) elevations resulting in an elevation adjustment of monitoring wells. The model domain was a 45 by 334 mesh with a finer mesh around the monitoring wells to ensure greater resolution at our area of interest. A specified flux

boundary was created on the upper surface of the model. This specified flux accounts for infiltration of precipitation and evapotranspiration. When the upper nodes are inundated by the tide the hydraulic head boundary condition changes to fluctuate with specified pressure (Evans and Wilson 2016). For salinity conditions, the solute flux across the upper boundary of the simulation domain depends on the boundary condition for fluid flow. Water entering the model through the specified fluid flux boundary condition has a salinity of zero, and water entering via the specified pressure boundary condition had a salinity of 35, representing the salinity of the tidal creek. Water leaving the upper surface via ET left its salt behind. The right and left boundary conditions for this model domain are placed at natural flow divides at Sapelo Island and are therefore modeled as no flow boundaries for fluid and solute transport.

The input for the model incorporated tidal data, precipitation information, evapotranspiration, and hydraulic properties, including porosity and saturated and unsaturated flow parameters. The test periods for calibration were June 1-23, 2020, and October 26, 2018- December 31, 2020. The simulated periods were chosen to include pronounced seasonal variations in salinity and water level. During this time period, the water table also had a clear response to precipitation events (Sanders 2021). The latter period was also helpful in comparing the simulated salinity with observed salinity because there were more salinity observations available for that time period. This model was run for five years from 2016-2020 to set initial conditions for subsequent calibration runs. In the first 5-year run, the salinity was initially set to 32 ppt for all nodes in the marsh platform and forest marsh boundary from 0-450 m from the creek, to initiate high

salinity conditions. Simulations showed that the choice of initial conditions mattered very little after a simulation time of only about 24 days, when the saltier water was flushed out of the high marsh. Even when precipitation was decreased by 50%, freshwater still permeated the upper marsh section.

In Sanders (2021), calibration issues arose that lead to permeabilities being set unrealistically high. To calibrate wells R2 in the marsh and R4 in the upland the permeability of the sand layer was set to a higher permeability than expected for a typical fine-grained sand. The simulated hydraulic head still did not match the observed trends as well as desired. Further analysis has shown that errors in estimating the elevation of land surface prevented some areas of the model from being inundated at the correct times. Some Van Genuchten parameters for unsaturated groundwater flow were also found to produce unrealistic retention curves. The overall objective of this research was to improve upon the modeling by Sanders (2021) in order to connect groundwater flow and salinity in salt marshes with disturbance through drought and sea level rise.

2.2 Model Construction

The numerical model presented in this paper was based on the model constructed by Sanders (2021). Many different data sets were collected to populate the input files needed for the SUTRA model to run. This includes tidal data from the USGS tidal gauge at Meridian, GA for recent 2016-2020 calibration runs as well as NOAA tidal data from Fort Pulaski, GA, which is the nearest tidal gauge with continuous records for 25 years of historical tidal data. The historical tidal levels from Fort Pulaski were raised by 0.33 m to match more recent records from Meridian. Precipitation data were collected from the

NERRS meteorological station at Marsh Landing located at Sapelo Island, GA (SAPMLMET). Hydraulic head data was collected at 15-minute intervals from the wells at Marsh Landing from August 2018 to March 2023 yet only data from August 2018 to December 2021 were used in this study. Salinity observations were collected by hand at irregular intervals from October 2018 to August 2022. Evapotranspiration rates in the preliminary model were set to a constant rate throughout all times of the day and year. We followed this approach in the current study, setting the evapotranspiration rate to 4 mm/day throughout the year, based on studies of Spartina-dominated salt marshes off the coast of Italy (Marani et al. 2006) and the Southeast coast of the US (Dacey and Howes 1984). We attempted to make a more realistic rate using the Turc equation with variables including temperature and total solar radiation (Hughes 2016, Turc 1961). The Turc equation was chosen based on data availability as well as mathematical simplicity, and the values ranged from about 3 mm/day to 9 mm/day depending on variables mentioned above. Changing the evapotranspiration rates to fluctuate daily caused major changes to in groundwater flow, in which the model did not correctly retain or drain water even after large precipitation events. Despite the quite different results in the simulated hydraulic head, these changes had very little effect on salinity. For simplicity, it was therefore decided to keep a constant rate of 4 mm/day throughout the simulation.

2.3 Calibration

The model was calibrated by comparing simulated water levels with observed water levels at Sapelo Island during April 1-30th, 2019. To determine the time period for calibration, we selected five time periods to test the model and visually assess sediment

property changes through various conditions. These test periods included a range of fluctuations in tidal water level, spring and neap variations, and varied precipitation events. The time periods were April 2019, July 15- Aug 13, 2019, March 2020 (March 1st - March 30th), May 2020 (May 1st to May 30th), and May 24 - June 22, 2020. Next we evaluated over 100 different combinations of permeability and porosity for the sediment layers, then selected the five most visually correlated modeled vs observed hydraulic head. The five visually correlated permeabilities chosen were then run through the five time periods, resulting in twenty-five combinations to show graphically how well the numerical model captures water level fluctuations due to hurricanes, drought, and spring/neap cycles. The time period selected to show our finalized hydraulic head results was April 2019 because this period captures spring and neap tidal cycles and had three clear precipitation events.

In addition to using the field data collected from Sanders (2021), additional core samples were taken in summer of 2022 at Sapelo Island near the monitoring well sites to improve sediment categorization (Figure 1.5C). Several sediment layer boundaries were adjusted compared to Sanders (2021) to change the sediment permeabilities above wells R2 and R3. These changes improved the draining of these wells, which helped the model match observed hydraulic head data. The boundaries of sediment layers within our model mesh, specifically the mud and crab burrowed mud, were adjusted to ensure the shallow wells at R2 and R3 are distinctly below these mentioned sediment layers (Figure 2.1). The sediment properties were estimated based on typical values for salt marsh sediments (Table 2.1).

Cores showed that Well R2 had only crab burrowed mud zone above the well screen, and R3 had only interbedded sand and mud above the well screen. The silty sand lens was added into the domain. Cores did not show the landward extent of this layer, but test runs showed no visible changes in salinity or groundwater flow whether the lens extended to the right most flow boundary or was limited to a narrower zone.

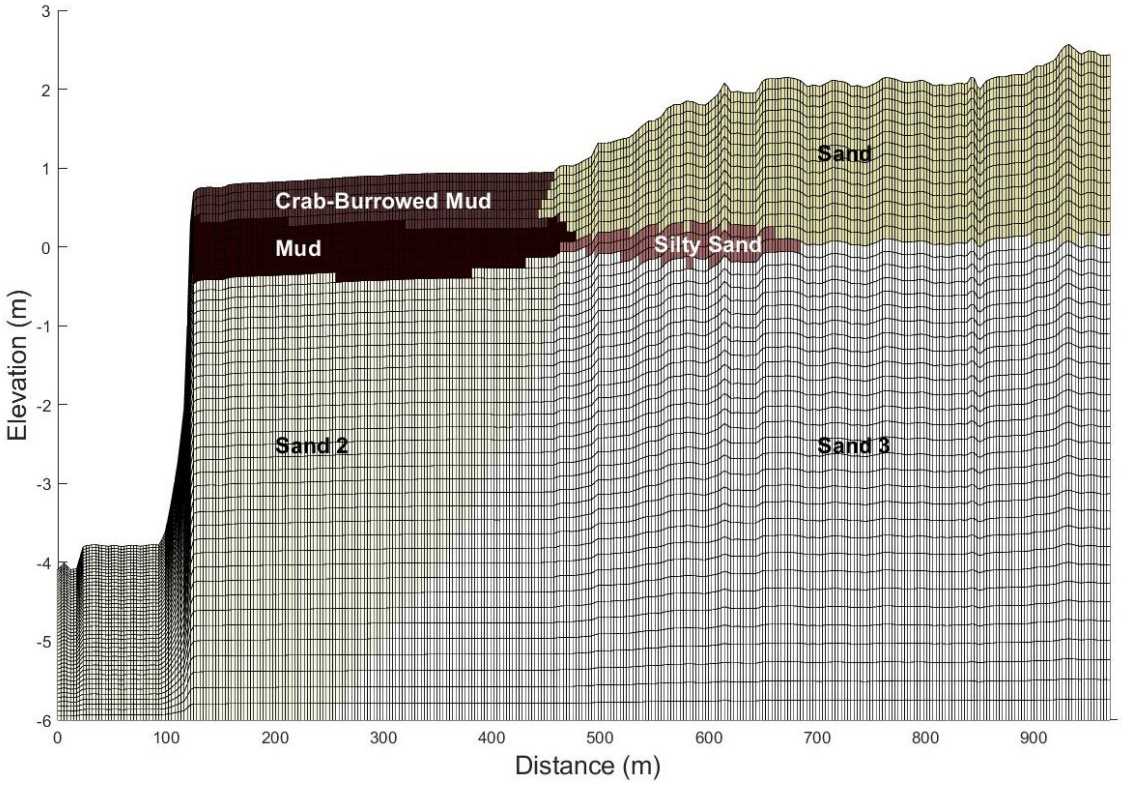

Figure 2.1: Model domain including polygons outlining sediment types, and white circles denoting well locations. The sediment types are described in Table 2.1.

Table 2.1: Classification of sediment types shown in Figure 2.1.

Sediment Classification	Permeability [m2] Maximum	Minimum	Porosity [-]
Sand	3.00E-10	3.00E-10	0.4
Crab Burrowed Mud	1.00E-12	1.00E-12	0.72
Mud	5.00E-13	5.00E-13	0.7
Silty Sand	1.00E-13	1.00E-13	0.43

The van Genuchten unsaturated flow parameters were updated from Sanders (2021) to match more typical water retention curves based on the models of Xiao et al. (2019) (Figure 2.2). The original parameters were estimated from Carsel and Parrish (1988), and the graphed water retention curves were not consistent with expected values (Carsel and Parrish 1988, Sanders 2021). In this study the van Genuchten parameters were estimated between the original and updated values shown in Xiao et al 2019 to keep the integrity of the original parameters from Carsel and Parish yet still have a realistic water retention curve. Using only the updated values from Xiao et al 2019 did not yield expected water level fluctuations with the sediments presented, which is why an estimation was used. Updating these parameters enabled the sediments to drain properly through model simulations, shown through more realistic fluctuations in the water level.

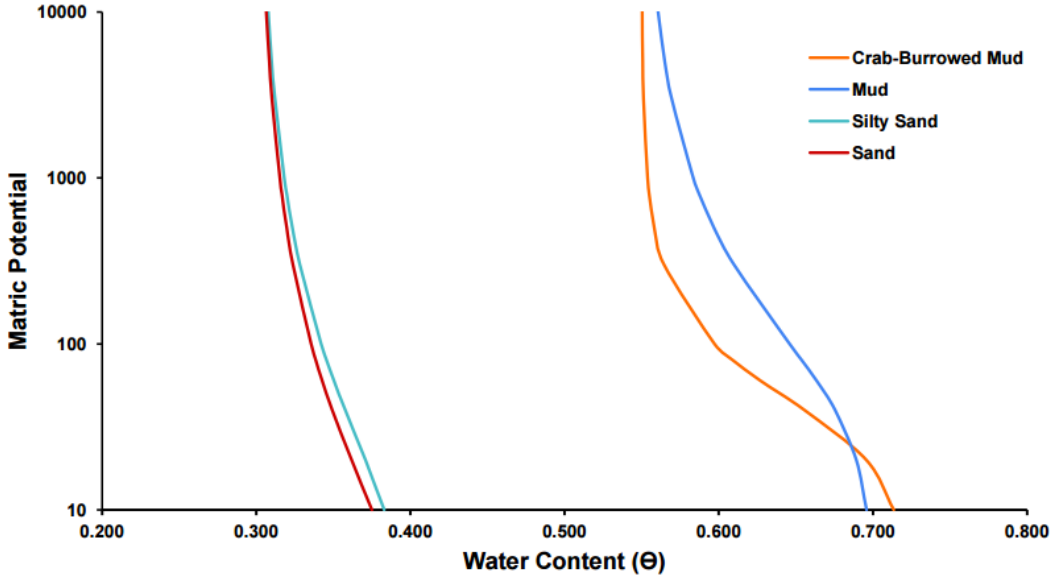

Figure 2.2: Water retention curves.

2.4 Monitoring and Simulating Salinity in Salt Marshes

Observed salinity data was collected at irregular intervals from 2018 to 2020, without a full range of seasons available to compare with simulated salinities (Figure A.5). While we do not expect simulated salinity values to exactly match field observations (Xiao et al 2019), the model reproduced observed trends in salinity and generated consistent data output which could be analyzed for trends over a range of time scales, from daily tidal cycles to seasonal variations. The salinity generated by the model was consistently lower than observed salinities by 6-29 ppt.

As will be shown below, the salinity generated by the numerical model reflects the influence of complex interactions between tides and rainfall, and it was difficult to identify the individual contributions of each physical process to changes in salinity. We used linear regression analyses to identify statistical correlations between the simulated salinity and the inputs of tides, precipitation, and the Palmer Drought Severity Index (PDSI). The tidal and precipitation data were calculated with a 30-day moving mean and PDSI is reported for each month. A multivariate linear regression was also completed with salinity vs all three dependent variables (tides, precipitation, and PDSI) but did not result in statistically significant results and showed no linear correlation.

CHAPTER 3: RESULTS

3.1 Stratigraphy

The sediments in the cores collected in summer of 2022 were distilled into four sediment types (Figure 3.1). The soil core measurements and sediment types were categorized then graphed on the same vertical scale as our model domain to ensure the sediment boundaries drawn in our model were at the correct elevation. We also found evidence of a silty sand lens starting in between R2 and R3 which likely extends into the upland (Figure 3.1). The sediment layers and types beyond the area where we collected sediment cores were approximated according to typical southeastern salt marsh stratigraphy. The calibrated sediment permeabilities are shown in Table 2.1.

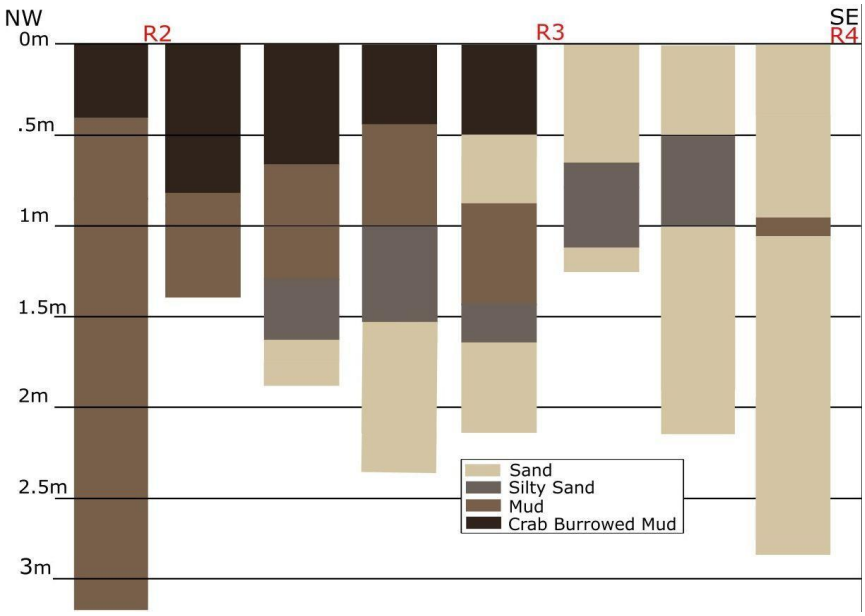

Figure 3.1: Soil stratigraphy chart estimated from soil cores taken June of 2022.

3.2 Hydraulic Head

For each of the twenty-five combinations of five time periods and five sets of permeability parameters a root mean squared error (RMSE) was calculated (Figure A.1). During the calibration phase of updating the model, RMSE showed that separating the sand layers into different zones was unnecessary and increased errors, so we assigned the same hydraulic properties to all sand in the model. Generally, when there was a large rainstorm with a simultaneous increase in water level in all our wells, the model seemed to reset itself in each time period. Although, there were significant rainstorms that did not cause widespread rises in the water table. Simulation results from April 2019 captured water level increases from the majority of rainstorms and high tides. The largest errors in the simulation concerned Well R4, where simulations underestimated the hydraulic head by as much as 20 cm during the drainage events after rainfall or a high tide. The drainage rate at R4 was nevertheless realistic, as indicated after rainfall by the slope of the hydraulic head during drainage events, shown from April 2-7, 7-16, and 20- 31 (Figure 3.2). The fit was generally much better for Wells R2 (Figure 3.2) and R3 (Figure 3.3), although the models underestimated the amount of drainage during long periods without tidal inundation. At R2 this was typically only 5 cm, but after long periods of drainage the simulated hydraulic head at R3 was as much as 10-15 cm higher than observed values. The model matched the observed hydraulic head at R2 and R3 very well during periods of frequent inundation.

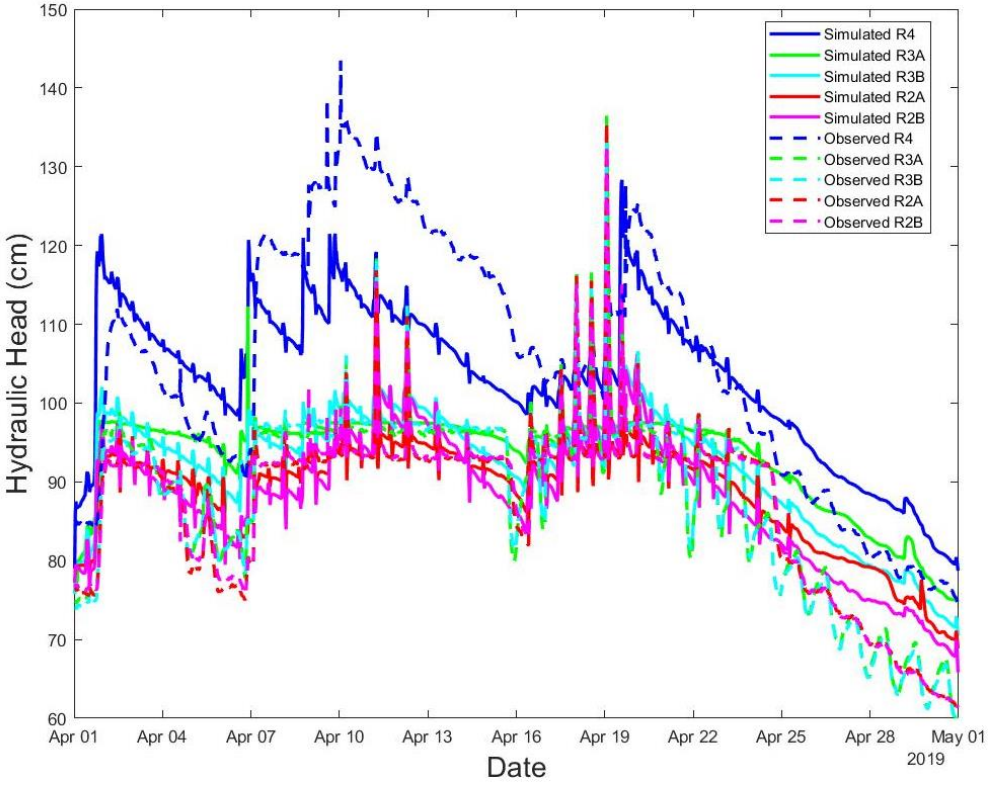

Figure 3.2: Observed and simulated hydraulic head values for April 2019.

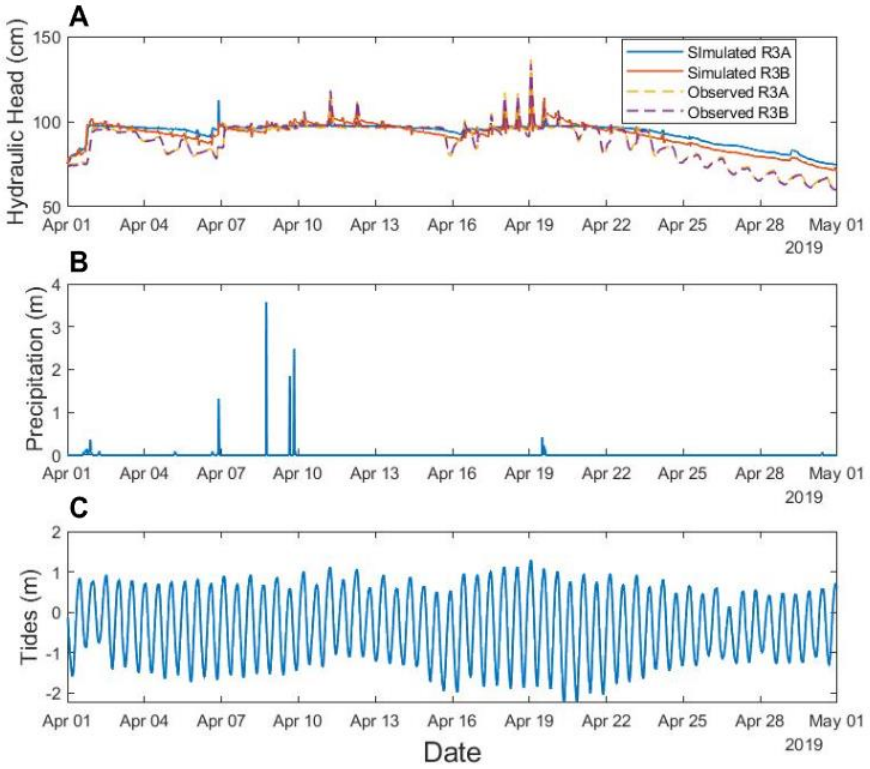

Figure 3.3: Simulated and observed hydraulic head at Well R3 with hydraulic forcing factors. (a) Simulated and observed hydraulic head measurements at Well R3. (b) Precipitation rate. (c) Tidal water level.

3.3 Salinity

The freshwater-saltwater interface or freshwater lens is a mixing zone area that migrates with varied tidal cycles and rainfall. The monitoring wells set up in this study were placed in the upper marsh to capture different sections of the freshwater lens. Well R2 and R3 located in the low marsh and hypersaline zones, respectfully, had the highest salinities with a strong influence from tidal fluctuations (Figure 3.4 a,c). Well R4 placed in the high marsh, had the lowest simulated salinities, only increasing with spring high tide events and significant rainfall (Figure 3.4). The sea level is higher during the summer/fall months, and at a minimum during the winter months (Figure 3.4 c). The higher tides during the summer and fall results in increased salinity and lower salinities in the winter (Gonneea et al. 2013, Wood and Harrington 2015). Modeled salinity values show a slow decrease in salinity from the fall into winter months of 2004, 2005, and 2006, then a sharp increase in salinity immediately following, which coincides with high mean water levels during a spring tide and decreased or smaller, insignificant precipitation events (Figure 3.4).

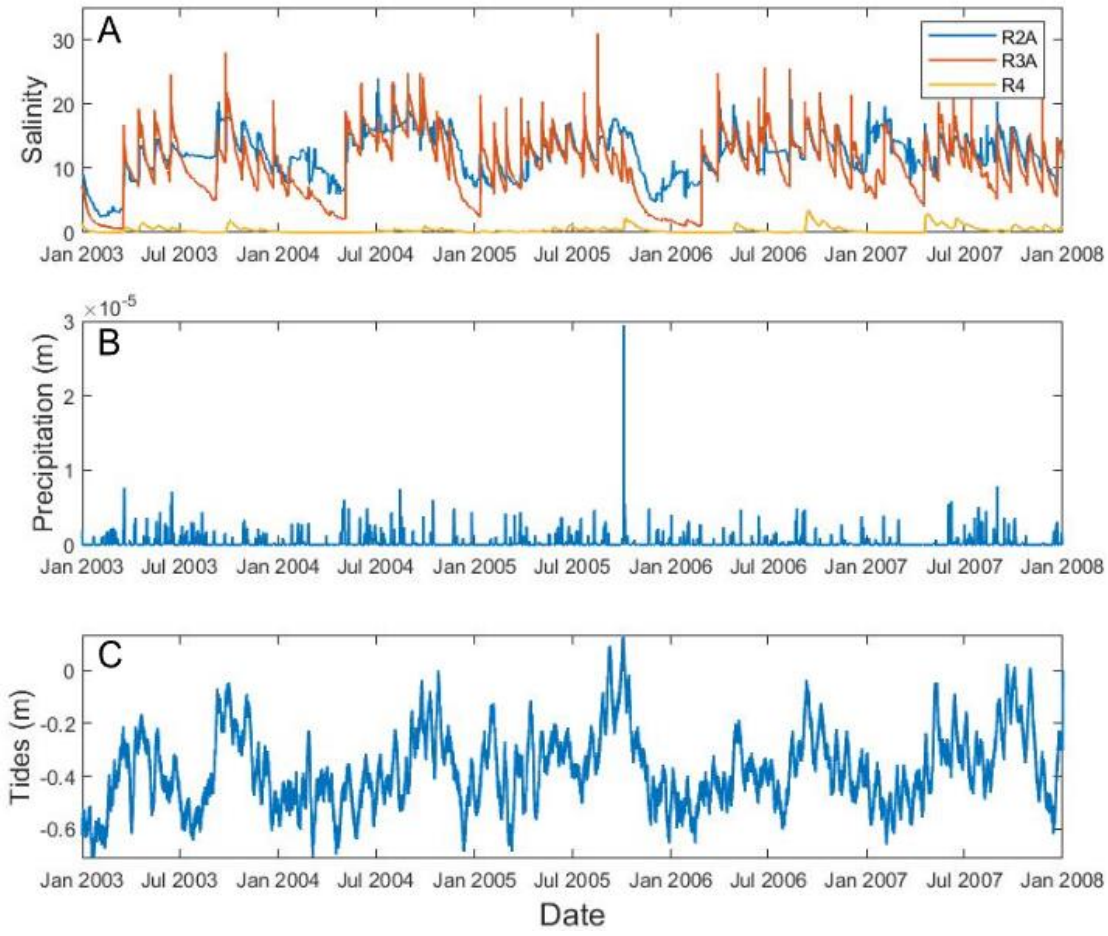

Figure 3.4: (a) Salinity at all three wells from 2003-2007. (b) Precipitation in meters. (c) Tides (30-day moving mean).

Simulated salinity from a 25-year period from 1998 to 2022 shows seasonal trends in salinity (Figure 3.5). Well R3A was chosen to represent salinity through this 25-year record since it can capture the contraction and expansion of the lens throughout varied groundwater fluctuations presented below. The simulated salinity values were smoothed using a moving mean averaged over 15 days to make the oscillation of salinity with seasonal trends and precipitation events more visible. Tides, evapotranspiration, and precipitation all fluctuate seasonally, especially in the upper marsh (Gardner et al. 2002). Increased hurricane activity and rainfall during hurricane season (June to November)

show large spikes in precipitation and the buildup of freshwater that contributes to freshening of the forest/marsh boundary during the winter in simulated salinity data. In simulations, prominent rainfall events during non-drought years in the summer/fall of 2005, 2009, and 2013 were followed by a large decrease in salinity the following winters approaching 0 ppt. The duration of freshening depended on the strength of the previous rainfall events (Figure 3.5). Salinity then increased during the summer/fall months.

During drought periods, high salinities persisted throughout the winter in annual trends in 1998- 2002, 2010-2013, and 2015-2018. This manifests as a long-term, consistent high salinity content without the normal winter freshening events. During the most notable drought from 1998-2002 (Figure 3.5), the salinity never fell below about 7 ppt. Throughout less severe drought periods from 2010-2013 and 2015-2018 the salinity remained higher than normal, despite slight freshening during winters. These short-term droughts cause an increase in minimum yearly salinity anywhere from 2-5 ppt, which returns to expected minimum salinity during the winters of non-drought years (Figure A.6). The lack of winter freshening during droughts suggests that less freshwater availability causes the freshwater lens to contract towards the upland with higher salinity propagating further in the high marsh.

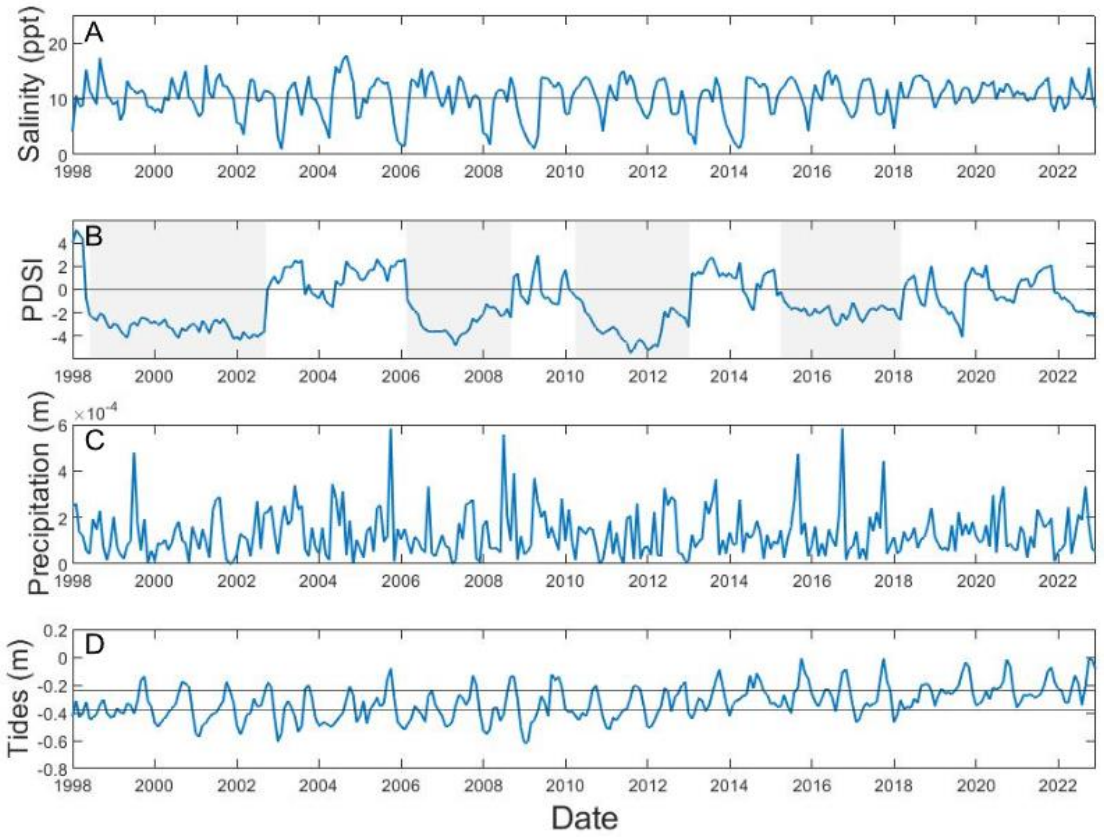

Figure 3.5: (a) Modeled salinity at Well R3A (15-day moving mean). Black line (y = 10.05) of average salinity from 2000-2010 for baseline. (b) Monthly PDSI values. Shaded regions indicate dry or drought conditions. (c) Monthly Precipitation from the Marsh Landing meteorological station. (d) Tides (30-day moving mean). Black line (y = 0.375) of average water level from 2000-2010 for baseline.

The pattern of seasonal variations in salinity appeared to change in 2018 (Figure 3.4a). Salinity remained high throughout this period, but there was no drought. Instead, sea level has remained high since 2018 (Figure 3.5c). Average sea level gradually rose about 0.13 m gradually from 2010 to 2022 based on a tidal average from 2000-2010 and 2018-2022. Long-term increase in mean water level or tidal amplitude increases the minimum salinity and over 5 years from 2018 to 2022 the minimum does not drop below

5.8 ppt, which under normal conditions is a higher-than-average minimum salinity (Figure A.6).

The freshwater lens movement is observed by contraction towards the upland during drought or high tides and expansion marshward during normal wet conditions or neap tides. The distribution of salinity changed to some degree over individual tidal cycles during a 24-hour period (Figure 3.6a, b) but significant migration of the freshwater lens occurred over longer time scales. For panels c through f in figure 3.6, average tidal conditions or were chosen to Seasonal variations caused tides to propagate further into the upland during the spring when sea level is higher (Figure 3.6c). In the winter there is an expansion of the freshwater/saltwater interface as well as wider salinity gradients in the mixing zone from 360-440 m compared to the spring (Figure 3.6d). During drought conditions in the spring there is a slight movement of higher salinity groundwater towards the upland (Figure 3.6e). Immediately following the drought period, the freshwater lens exhibits a longer mixing zone from 360-470 m in the winter as well as extended salinity gradients (Figure 3.6f).

The completion of three linear regression analyses revealed that in smaller 5-year periods, tides (averaged on a 15-day scale) have the main influence on salinity changes with a p-value < .05. In each of the 5-year time periods when run separately, the tidal signal has the highest R^2 value of about 0.25 for each section. When doing a regression analysis with the full 20 years, tides had the most significant correlation with salinity (p = 9.64E-12), yet PDSI was also significant (p = 0.01) (Table 3.1). With a positive correlation for tides and salinity, as the salinity increased, tidal signals also increased. Since PDSI was usually not significant during the smaller 5-year model runs, yet

significant during the 25-year run, this suggests that PDSI affects salinity on a longer time scale, while tides are significant through smaller and larger time scales.

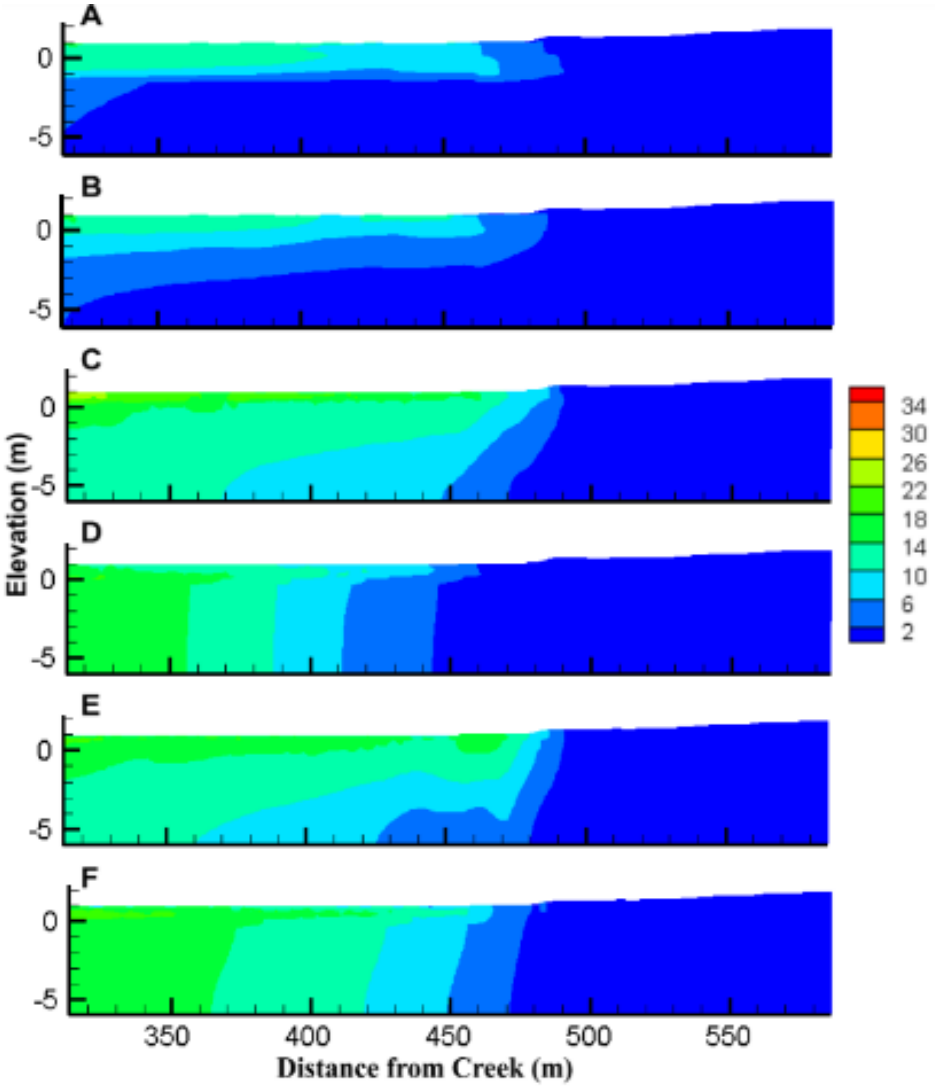

Figure 3.6: Plot of modeled salinity at the forest/marsh boundary from 315 m to 585 m. Panels C-F are plots during an average tidal period. (a) Low tide. (b) High tide. (c) Spring in April 2005. (d) Winter in December 2005. (e) First month of 1998-2002 drought in May 1998. (f) First month after drought in November 2002.

Table 3.1: Linear regression analysis of salinity with the variable's precipitation, tides, and PDSI with 25-year period.

Variable	R-Square	p-Value	RMSE
Precipitation	0.01	0.10	3.32
Tides	0.14	9.64E-12	3.09
PDSI	0.02	0.01	3.31

CHAPTER 4: DISCUSSION

The results from this study indicate that salinity is strongly influenced by variations in mean water level, particularly seasonal variations, as well as drought conditions. We also found that pulse and press disturbances affect salinity differently. Drought caused increases in the minimum simulated salinity, which caused a temporary variation from normal seasonal variations. Simulation results suggested that drought lasting longer than a year has no lasting effects on salinity after the end of the drought, yet after 0.13 m sea level rise there is a seemingly permanent increase in salinity in the mid marsh.

4.1 Model Performance Relative to Field Observations

Simulated salinity was anywhere from 6-29 ppt lower when compared to observed salinities. Obvious ways to increase the salinity in the simulations are to increase ET and decrease discharge of fresh groundwater from the upland, but when implemented these changes had very little impact on the simulated salinities. We abandoned further attempts to match observed salinities in light of previous work by Xiao et al. (2019), who noted that macropores associated with crab burrows and plant roots significantly complicate both measurement and simulation of salinity in the root zone. In the field, tension samplers access porewaters with much shorter residence times than diffusion samplers, which can lead to differences in salinity obtained by the two methods (Harvey and Nuttle, 1995; Xiao et al., 2019). Thus it is not entirely clear what salinity

should be reported as representative for the root zone, and it is even less clear how that salinity might relate to salinities obtained from monitoring wells such as we used (a third sampling method). At the same time, standard groundwater flow modeling approaches do not account for rapid transport through preferential flow paths and may underestimate the input of salinity across the marsh surface (Xiao et al., 2019). In the end, uncertainties with respect to field sampling and simplifications made in modeling make it very difficult to describe the degree to which a simulation represents a specific field site. We expect that matching observed salinities in salt marshes using numerical models will require a continuous sampling method in the field combined with numerical models that include dual-medium approaches or, at the very least, enhanced solute transport across the marsh surface via an effective dispersion term. In the meantime, our simplified models revealed important trends and seasonal patterns in salinity without the added expense of major field instrumentation or complex modeling approaches.

4.2 Salinity and Ecological Change in Salt Marshes

The results from the linear analyses show that mean water levels are the main influence of salinity throughout the marsh, with respect to seasonal variations as well as long-term sea level rise. This may seem to conflict with the obvious connections between drought and plant zone migration presented in Figure 1.4, which suggest that drought should be a major control on salinity. These two sets of information can be reconciled by noting that, while drought is a secondary control on salinity in the high marsh, drought interrupts normal patterns of winter freshening, which in turn appears to be a major control on plant zone migration. Thus, although ecological surveys commonly focus on

soil conditions during the growing season, this work suggests that conditions during the winter or very early growing season should be investigated as a possible control on plant zonation.

In our simulations, pulse disturbances did not have a long-lasting (more than one year) effect on the salinity. For example, after long-term droughts, the salinity resumed normal seasonal changes the next year (Figure 3.5). Even during short-term droughts, the simulations showed occasional seasonal freshening in the winter in the high marsh, indicating a reasonably quick (months) response of salinity to changes in precipitation. This not only brings insight into the time-scales for variability of salinity in the root zone but also indicates that the continual increase in simulated salinity starting in 2018 could not have been caused by drought. Instead we note a gradual rise in sea level from 2018-2022 (Figure 3.4C), which likely indicates the freshwater-saltwater boundary is moving inland. The loss of seasonal variations in salinity during a 5-year period with no notable wet or drought conditions suggest a long-term transition at R3 from a high marsh hydrologic zone, where the freshwater lens plays an important role, into a mainly tidally dominated lower marsh zone.

The fact that salinity returned to normal seasonal patterns immediately after droughts ended also sheds light on the way plant zones respond to drought. The long-term study from GCE LTER observed showed a permanent retreat of *Juncus* inland from study plots during drought, whereas *Spartina* cover decreased only temporarily during the drought (S. Pennings, *pers. comm.*). This suggests that established patches of Juncus can persist in increasingly stressful conditions, but once displaced during drought it cannot re-establish itself under those conditions. The decline in *Spartina* cover, accompanied by

a gain in *Batis* and *Sarcocornia*, clearly indicates stressful conditions for *Spartina* during the drought, but *Spartina* was able to recover once drought conditions ended.

CHAPTER 5: CONCLUSION

This study was designed to investigate the possibility that salt marsh migration was caused by changes in salinity and to find out whether this represented a sustained change in groundwater. We expected precipitation to be a major control on salinity, but our simulations suggested instead that mean water level was the main driver for salinity in the high marsh, because low mean water levels in winter allowed the freshwater lens to expand seasonally. Our simulations showed that drought limited normal seasonal variations in salinity, which likely triggered migration of plant zones, but drought did not cause long-term changes in salinity overall. Landward migration of the freshwater-saltwater interface due to sea level rise was very small compared to migration due to seasonal variations and drought in the high marsh. Nevertheless, we found that seasonal variations in salinity ceased at R3 after 2018, indicating that sea level rise had progressed far enough that the site was no longer affected by interactions with the freshwater lens.

This modeling study shows the complexity of interactions between tidal cycles, precipitation, and various types of disturbances that influence salinity. The sediment properties were improved from previous model simulations, but some simplifications were retained, particularly in the stratigraphy. We did not sample further than 2 m underground, so additional sand and mud layers from previous migrations may be present in the subsurface. More complex dual-porosity models could be more useful in the future to capture preferential flow and transport through crab burrows and other macropores.

Despite the limitations of a simple 2D numerical model, this groundwater model identified key seasonal variations and long-term trends in salinity and is useful in determining a baseline for salinity and flow patterns for future work.

The study site for this model on Sapelo Island is a protected area free of many anthropogenic barriers near salt marshes and limited structures in general. It is important to observe how these protected areas are affected by disturbance and sea level rise to use as a baseline for research studying less pristine salt marshes in the Southeast. The research presented in this paper could be expanded by creating and comparing a numerical model based on a salt marsh with different topography or human influence in the area.

WORKS CITED

Burns, C. J., M. Alber, and C. R. Alexander. 2021. Historical Changes in the Vegetated Area of Salt Marshes. Estuaries and Coasts 44:162–177.

Dacey, J. W. H., and B. L. Howes. 1984. Water Uptake by Roots Controls Water Table Movement and Sediment Oxidation in Short Spartina Marsh. Science 224:487–489.

Evans, T. B., and A. M. Wilson. 2016. Groundwater transport and the freshwater–saltwater interface below sandy beaches. Journal of Hydrology 538:563–573.

Fagherazzi, S., G. Mariotti, P. Wiberg, and K. McGlathery. 2013. Marsh Collapse Does Not Require Sea Level Rise. Oceanography 26:70–77.

Gardner, L. R., and D. E. Porter. 2001. Stratigraphy and geologic history of a southeastern salt marsh basin, North Inlet, South Carolina, USA. Wetlands Ecology and Management 9:371–385.

Gardner, L. R., H. W. Reeves, and P. M. Thibodeau. 2002. Groundwater dynamics along forest-marsh transects in a southeastern salt marsh, USA: Description, interpretation and challenges for numerical modeling. Wetlands Ecology and Management 10:143–157.

Goñi, M. A., and I. R. Gardner. 2003. Seasonal Dynamics in Dissolved Organic Carbon Concentrations in a Coastal Water-Table Aquifer at the Forest-Marsh Interface. Aquatic Geochemistry 9:209–232.

Gonneea, M. E., A. E. Mulligan, and M. A. Charette. 2013. Climate-driven sea level anomalies modulate coastal groundwater dynamics and discharge. Geophysical Research Letters 40:2701–2706.

Harvey, J. W., and W. K. Nuttle. 1995. Fluxes of water and solute in a coastal wetland sediment. 2. Effect of macropores on solute exchange with surface water. Journal of Hydrology 164:109–125.

Hughes, A. L. H., A. M. Wilson, and J. T. Morris. 2012. Hydrologic variability in a salt marsh: Assessing the links between drought and acute marsh dieback. Estuarine, Coastal and Shelf Science 111:95–106.

Kirwan, M. L., and J. P. Megonigal. 2013. Tidal wetland stability in the face of human impacts and sea-level rise. Nature 504:53–60.

Li, F., and S. C. Pennings. 2019. Response and Recovery of Low-Salinity Marsh Plant Communities to Presses and Pulses of Elevated Salinity. Estuaries and Coasts 42:708–718.

Marani, M., S. Silvestri, E. Belluco, N. Ursino, A. Comerlati, O. Tosatto, and M. Putti. 2006. Spatial organization and ecohydrological interactions in oxygen-limited vegetation ecosystems. Water Resources Research 42.

Miklesh, D., and C. Meile. 2018. Porewater salinity in a southeastern United States salt marsh: Controls and interannual variation. PeerJ 6:e5911.

Moffett, K. B., S. M. Gorelick, R. G. McLaren, and E. A. Sudicky. 2012. Salt marsh ecohydrological zonation due to heterogeneous vegetation–groundwater–surface water interactions. Water Resources Research 48.

Morris, J. T. 1995. The Mass Balance of Salt and Water in Intertidal Sediments: Results from North Inlet, South Carolina. Estuaries 18:556–567.

Morris, J. T., P. V. Sundareshwar, C. T. Nietch, B. Kjerfve, and D. R. Cahoon. 2002. Responses of Coastal Wetlands to Rising Sea Level. Ecology 83:2869–2877.

Pennings, S. C., and R. M. Callaway. 1992. Salt Marsh Plant Zonation: The Relative Importance of Competition and Physical Factors. Ecology 73:681–690.

Pennings, S. C., M.-B. Grant, and M. D. Bertness. 2005. Plant zonation in low-latitude salt marshes: disentangling the roles of flooding, salinity and competition. Journal of Ecology 93:159–167.

Pennings, S. C., and C. L. Richards. 1998. Effects of wrack burial in salt-stressed habitats: Batis maritima in a southwest Atlantic salt marsh. Ecography 21:630–638.

Sanders, S. C. 2021. Groundwater Flow and Transport at the Forest-Marsh Boundary: A Modeling Study:53.

Solohin, E., S. E. Widney, and C. B. Craft. 2020. Declines in plant productivity drive loss of soil elevation in a tidal freshwater marsh exposed to saltwater intrusion. Ecology 101:e03148.

Vitola, I., V. Vircavs, K. Abramenko, D. Lauva, and A. Veinbergs. 2012. Precipitation and Air Temperature Impact on Seasonal Variations of Groundwater Levels. Environmental and Climate Technologies 10:25–33.

Turc L., 1961. Estimation of irrigation water requirements, potential evapotranspiration: a simple climatic formula evolved up to date. Annals of Agronomy 12: 13-49

Voss, C. I., and A. M. Provost. 2002. SUTRA: A model for 2D or 3D saturated-unsaturated, variable-density ground-water flow with solute or energy transport. Page Water-Resources Investigations Report. U.S. Geological Survey.

Wilson, A. M., T. Evans, W. Moore, C. A. Schutte, S. B. Joye, A. H. Hughes, and J. L. Anderson. 2015. Groundwater controls ecological zonation of salt marsh macrophytes. Ecology 96:840–849.

Wilson, A. M., and L. R. Gardner. 2006. Tidally driven groundwater flow and solute exchange in a marsh: Numerical simulations. Water Resources Research 42.

Wilson, A. M., W. S. Moore, S. B. Joye, J. L. Anderson, and C. A. Schutte. 2011. Storm-driven groundwater flow in a salt marsh. Water Resources Research 47.

Wilson, A., M. Shanahan, and E. Smith. 2021. Salt Marshes as Groundwater Buffers for Development: A Survey of South Carolina Salt Marsh Basins. Frontiers in Water 3.

Wood, C., and G. A. Harrington. 2015. Influence of Seasonal Variations in Sea Level on the Salinity Regime of a Coastal Groundwater–Fed Wetland. Groundwater 53:90–98.

Xiao, K., A. M. Wilson, H. Li, and C. Ryan. 2019. Crab burrows as preferential flow conduits for groundwater flow and transport in salt marshes: A modeling study. Advances in Water Resources 132:103408.

Xin, P., B. Gibbes, L. Li, Z. Song, and D. Lockington. 2010. Soil saturation index of salt marshes subjected to spring-neap tides: a new variable for describing marsh soil aeration condition. Hydrological Processes 24:2564–2577.

APPENDIX A: AUXILLARY FIGURES

Table A.1: Average RMSE for all wells for 5 time periods noted in the left column. Permeability 2 is only sand in the top portion of upland as 3.0E-10 and others at 1.0E-10. Permeability 2 is all sand sediments with a permeability of 3.0E-10. Permeability 3 is only sand in the top portion of upland as 4.0E-10 and others at 1.0E-10. Permeability 4 is only sand in the top portion of upland as 8.0E-10 and others at 1.0E-10. Permeability 5 is sand in the top portion of upland as 3.0E-10 and sand under the low marsh as 5.0E-10 others at 1.0E-10.

Time Period	Permeability	Average RMSE
April 2019	1	53.01
	2	47.42
	3	47.49
	4	50.43
	5	53.43
July 15- Aug 13,2019	1	16.78
	2	13.08
	3	13.56
	4	13.69
	5	13.18
March 2020	1	15.77
	2	11.80
	3	14.72
	4	16.79
	5	17.61
May 2020	1	9.52
	2	7.63
	3	8.61
	4	8.22
	5	8.49
May 24 - June 22, 2020	1	10.57
	2	9.13
	3	9.21
	4	9.22
	5	9.69

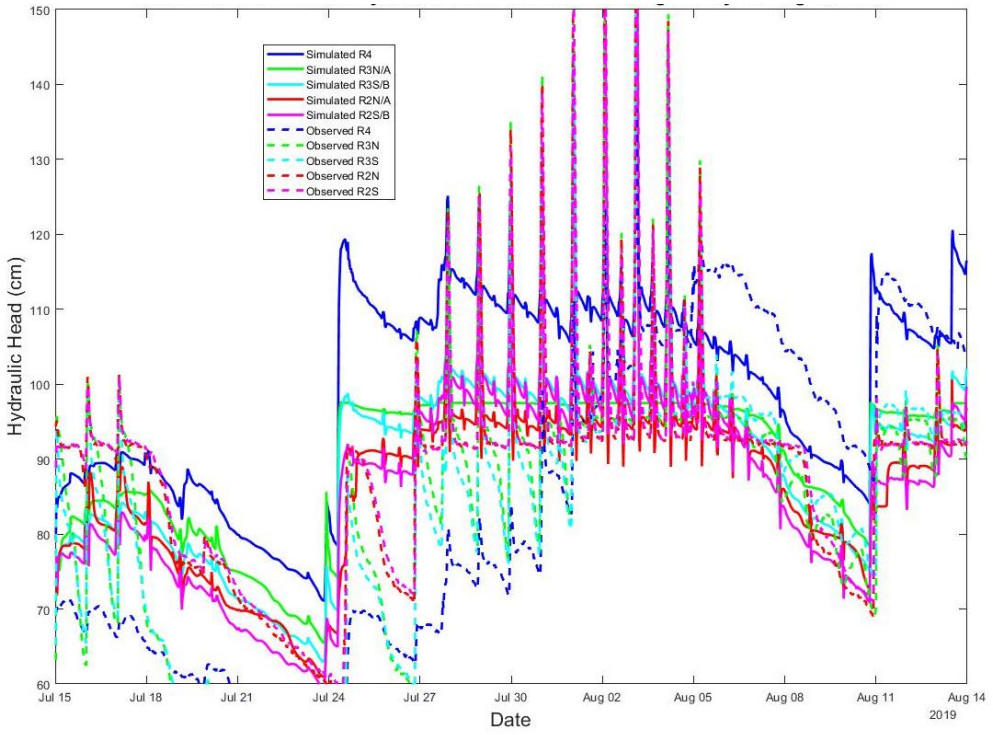

Figure A.1: Simulated vs observed hydraulic head during time period 2, July 15 - August 13th, 2019, with permeability group 2.

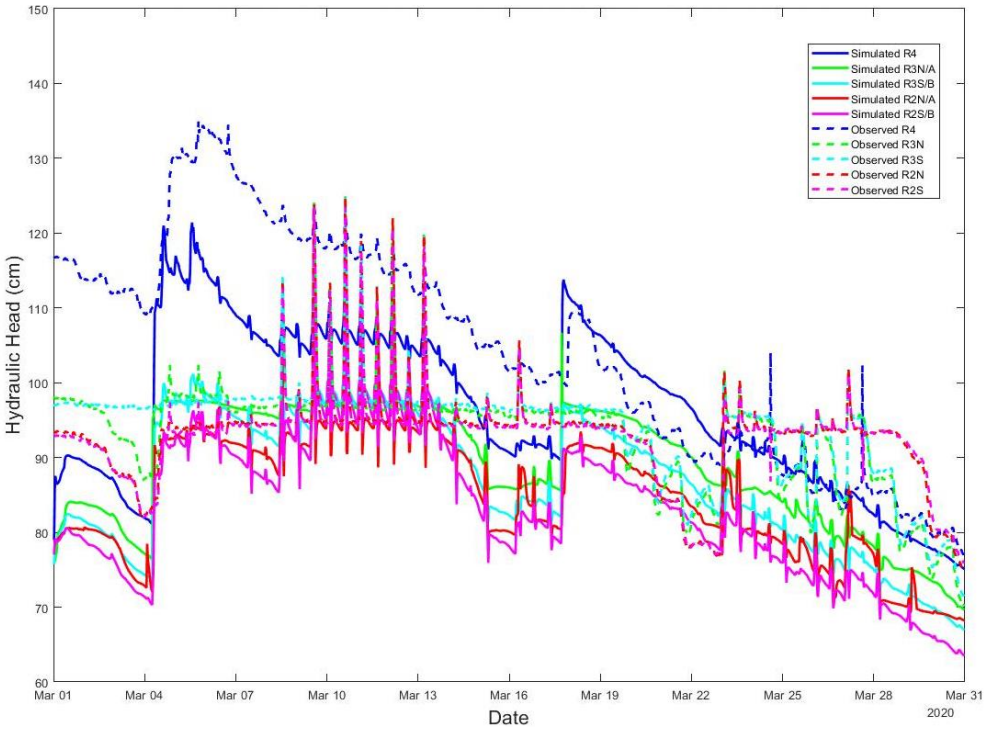

Figure A.2: Simulated vs observed hydraulic head during time period 3, March 2020 with permeability group 2.

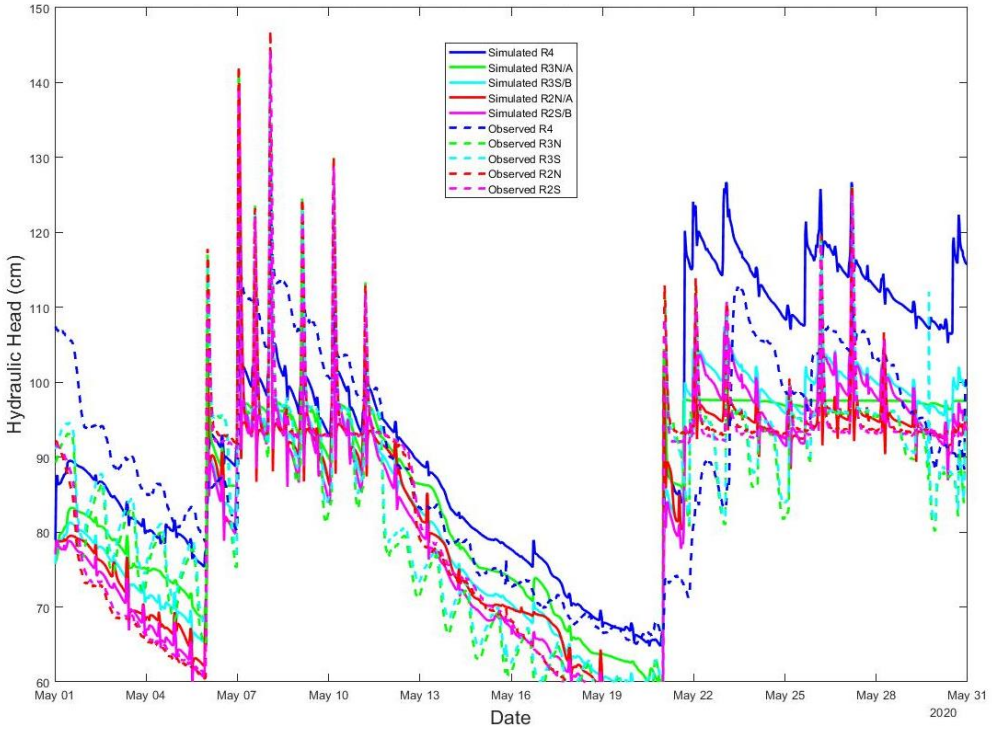

Figure A.3: Simulated vs observed hydraulic head during time period 4, May 2020 with permeability group 2.

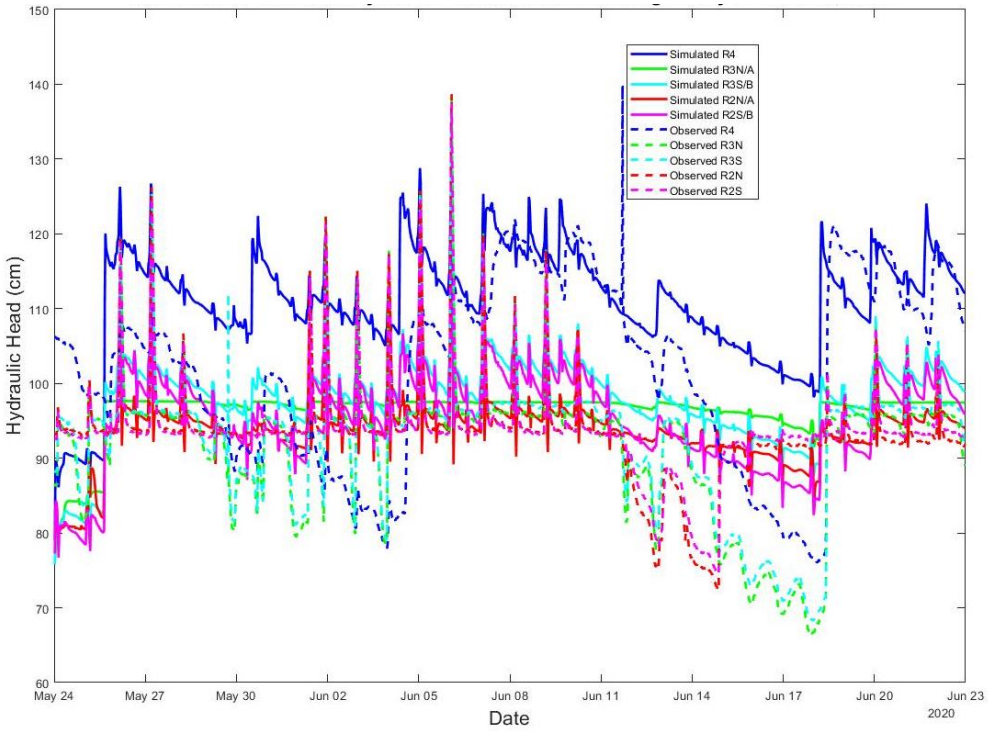

Figure A.4: Simulated vs observed hydraulic head during time period 5, May 24th - June 22nd, 2020, with permeability group 2.

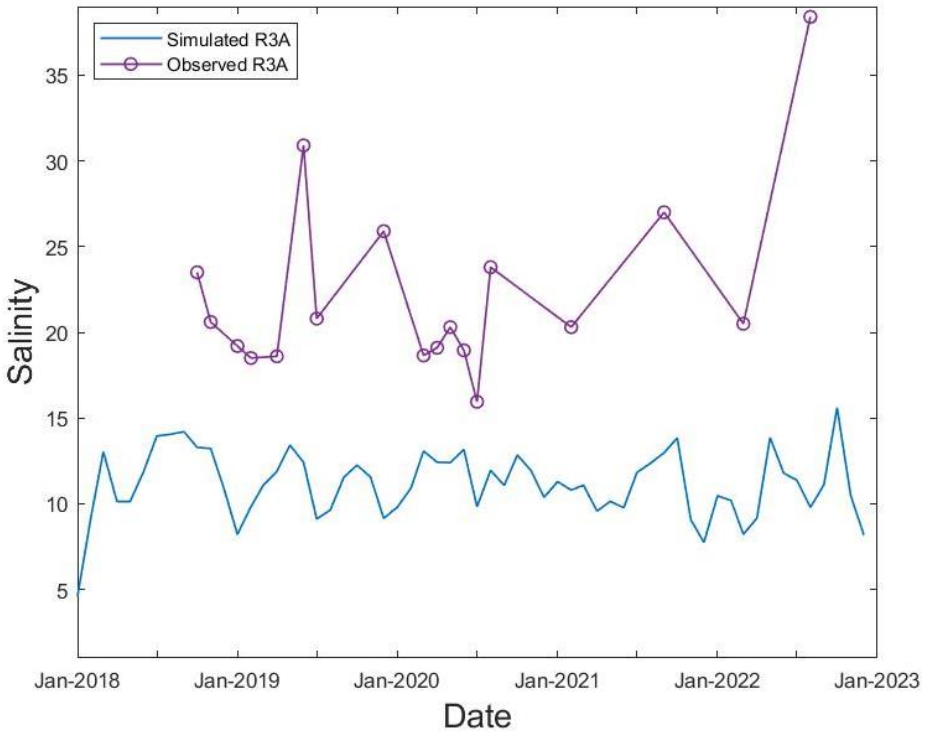

Figure A.5: Simulated vs Observed salinity at well R3A from 2018-2022.

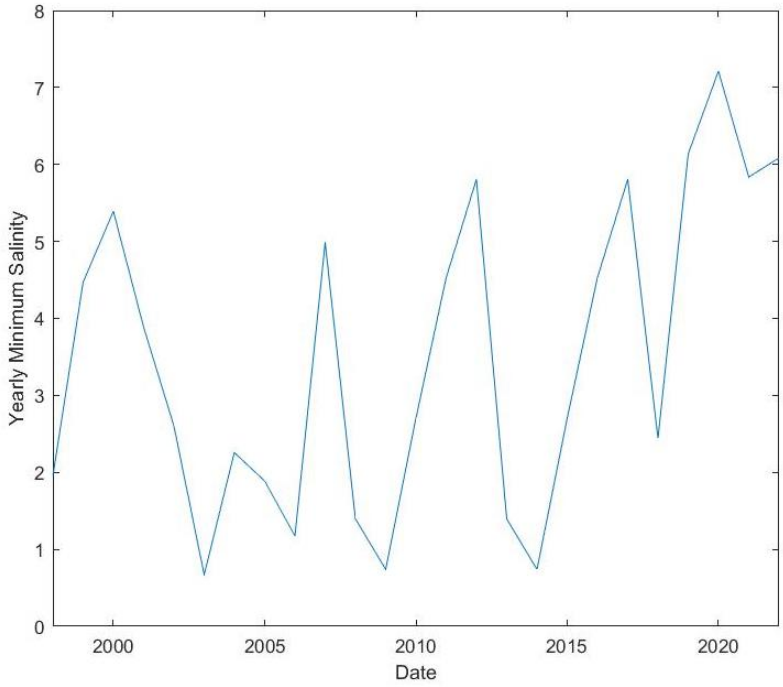

Figure A.6: Yearly minimum salinity from 1998-2022

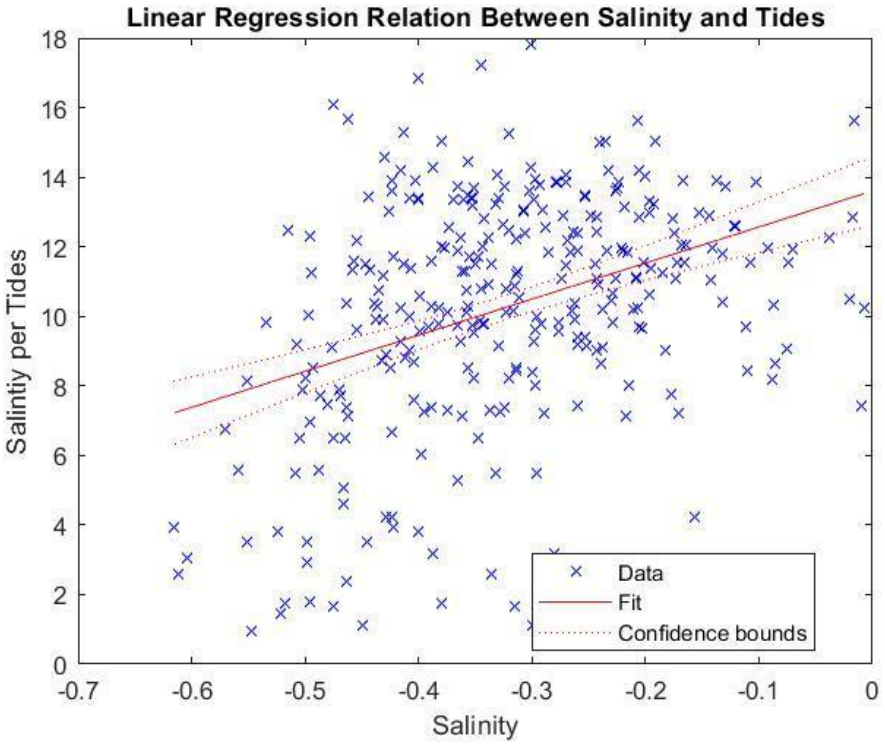

Figure A.7: Linear regression model results of salinity and tides

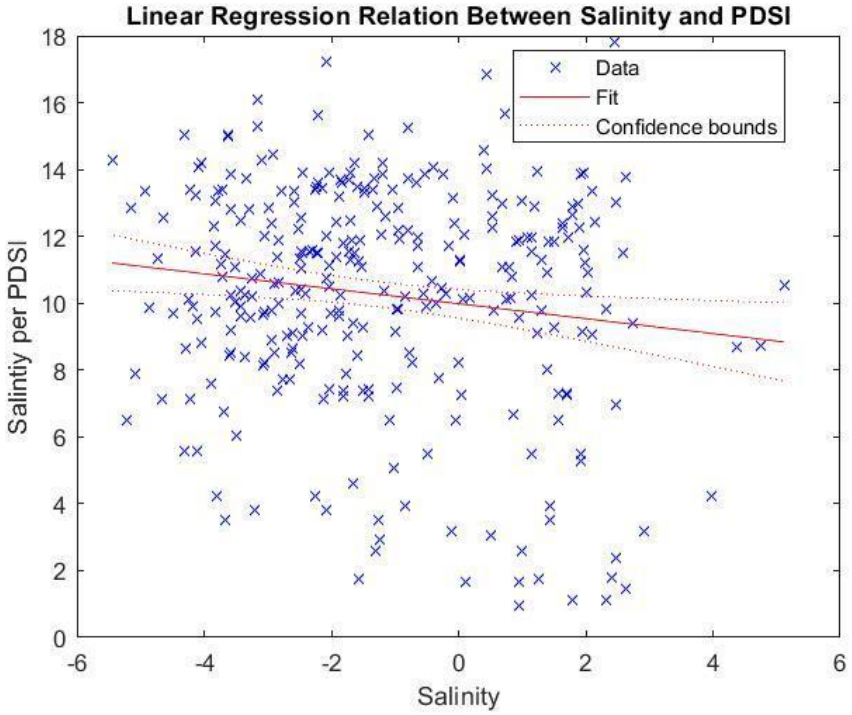

Figure A.8: Linear regression model results of salinity and PDSI.

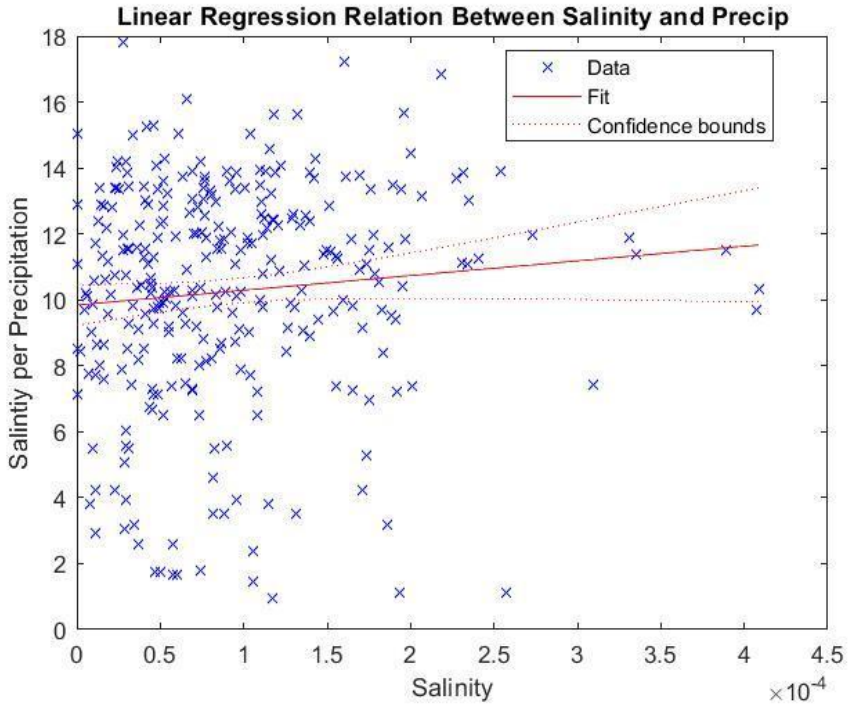

Figure A.9: Linear regression model results of salinity and precipitation

Table A.2: Van Genuchten Parameters

Soil Texture	Θs (porosity)	Θr	Ks (cm/hour)	Alpha	n	m
Crab Burrowed Mud	0.72	0.55	3.31E-03	0.03	2.12	0.53
Mud	0.7	0.55	1.66E-03	0.02	1.5	0.33
Silty Sand	0.4	0.30	3.31E-01	0.1	1.37	0.27
Sand	0.4	0.30	3.31E-01	0.16	1.37	0.27

Table A.3: Saturated Flow Parameters

Parameter	Symbol	Soil Type			
		Crab-Burrowed Mud	Mud	Silty Sand	Sand
Porosity	Θs	0.72	0.7	0.4	0.4
Residual Water Content	Θr	0.55	0.55	0.30	0.30
Hydraulic Conductivity	Ks	3.31E-03	1.66E-03	3.31E-01	3.31E-01
Capillary Rise	α	0.03	0.02	0.10	0.16
Grain Size	*n*	2.12	1.5	1.37	1.37